PUCHI regulates very long chain fatty acid biosynthesis during lateral root and callus formation

Duy-Chi Trinh[a,b], Julien Lavenus[a,c], Tatsuaki Goh[d], Yohann Boutté[e], Quentin Drogue[a], Virginie Vaissayre[a], Frédérique Tellier[f], Mikaël Lucas[a], Ute Voß[c], Pascal Gantet[a], Jean-Denis Faure[f], Stéphane Dussert[a], Hidehiro Fukaki[g], Malcolm J. Bennett[c], Laurent Laplaze[a,1], and Soazig Guyomarc'h[a,1]

[a]Unité Mixte de Recherche (UMR) Diversité Adaptation et Développement des Plantes, Institut de Recherche pour le Développement, Université de Montpellier, 34394 Montpellier Cedex 5, France; [b]Department of Pharmacological, Medical and Agronomical Biotechnology, University of Science and Technology of Hanoi, Cau Giay District, Hanoi, Vietnam; [c]University of Nottingham, Sutton Bonington, Loughborough LE12 5RD, United Kingdom; [d]Graduate School of Science and Technology, Nara Institute of Science and Technology, Ikoma, Nara 630-0192, Japan; [e]Laboratoire de Biogénèse Membranaire, UMR 5200, CNRS, Université de Bordeaux, 33882 Villenave d'Ornon Cedex, France; [f]Institut Jean-Pierre Bourgin, UMR 1318, Institut National de la Recherche Agronomique, AgroParisTech, CNRS, Université Paris-Saclay, 78026 Versailles Cedex, France; and [g]Department of Biology, Graduate School of Science, Kobe University, Kobe 657-8501, Japan

Edited by Ottoline Leyser, University of Cambridge, Cambridge, UK, and approved June 4, 2019 (received for review April 16, 2019)

Lateral root organogenesis plays an essential role in elaborating plant root system architecture. In *Arabidopsis*, the AP2 family transcription factor PUCHI controls cell proliferation in lateral root primordia. To identify potential targets of PUCHI, we analyzed a time course transcriptomic dataset of lateral root formation. We report that multiple genes coding for very long chain fatty acid (VLCFA) biosynthesis enzymes are induced during lateral root development in a PUCHI-dependent manner. Significantly, several mutants perturbed in VLCFA biosynthesis show similar lateral root developmental defects as *puchi-1*. Moreover, *puchi-1* roots display the same disorganized callus formation phenotype as VLCFA biosynthesis-deficient mutants when grown on auxin-rich callus-inducing medium. Lipidomic profiling of *puchi-1* roots revealed reduced VLCFA content compared with WT. We conclude that PUCHI-regulated VLCFA biosynthesis is part of a pathway controlling cell proliferation during lateral root and callus formation.

lateral root formation | morphogenesis | VLCFA | callus formation | cell division

Plant root system architecture (RSA) is the 3D configuration of a whole root system in its living environment (1). It is a major determinant of plant viability and crop yield, and a target for breeding to improve crop performance under various stresses (2, 3). Root branching is of particular importance because it largely determines the overall surface area of the root system and its spatial organization in the soil. The molecular mechanisms of root branching have been extensively studied in the model plant *Arabidopsis thaliana*. Lateral roots (LRs) originate from a small group of xylem-pole pericycle cells of the primary root that are primed by auxin to acquire founder cell identity (4). These founder cells undergo a succession of anticlinal and periclinal cell divisions that eventually result in the formation of a dome-shaped lateral root primordium (LRP; refs. 5–8). The LRP emerges through overlaying root tissues to become a LR (9).

Lateral root development is an excellent experimental system to study de novo meristem formation (10). Moreover, recent studies have shown that lateral root formation shares common mechanisms with organ regeneration in tissue culture, especially the first step of callus formation (11–14). While many genes involved in lateral root development have been identified, little is known about the mechanisms that progressively organize the LRP into a new root meristem (15). LRP organization is not dependent on a stereotypical cell division pattern and therefore on cell lineage (6, 7). It is a dynamic process dependent on complex gene regulatory networks and on cell–cell interactions including hormonal and biomechanical signals (6, 9, 16). Interestingly, inference of the gene regulatory network involved in LR formation suggested an early patterning mechanism defining the central region and flanks of the LRP and identified genes involved in this process (17). One such gene encodes the AP2/EREBP family transcription factor PUCHI, which was previously shown to control cell proliferation during LRP formation (18). The *puchi-1* mutant LRP exhibits additional anticlinal and periclinal cell divisions from early stages and produces abnormally enlarged flank cells (18). However, little is known about the pathways that are regulated by PUCHI.

Very long chain fatty acids (VLCFAs) are fatty acids with 20 or more carbons synthesized in the endoplasmic reticulum from long chain-fatty acyl-CoA (16 or 18 carbons) by the fatty acid elongase complex (*SI Appendix*, Fig. S1). This complex catalyzes rounds of two-carbon elongation in a four-step mechanism, involving a 3-ketoacyl-CoA synthase (KCS), a 3-ketoacyl-CoA reductase (KCR), a 3-hydroxyacyl-CoA dehydratase (HACD), and a trans-2,3-enoyl-CoA reductase (ECR). Multiple KCS enzymes with various expression patterns have been described, and their substrate affinity is thought to be responsible for the final VLCFA chain length (19–21). In contrast, only a limited number of genes that encode functional enzymes catalyzing each of the subsequent steps of the elongation cycle has been identified in *Arabidopsis*. *KETOACYL REDUCTASE 1* (*KCR1*) encodes an *Arabidopsis* KCR enzyme (22). *PASTICCINO 2* (*PAS2*; ref. 23) and *PROTEIN TYROSINE PHOSPHATASE-like* (*PTPLA*)

Significance

Lateral root organogenesis enables plant roots to branch and improve foraging for resources. Using a systems biology approach, we discovered expression of very long chain fatty acid (VLCFA) biosynthesis pathway genes are induced downstream of PUCHI, a transcription factor controlling cell division and morphogenesis during lateral root formation. Furthermore, we report that regulation of the VLCFA biosynthesis pathway by PUCHI is conserved for both lateral root development and callus formation, the first step in in vitro plant regeneration.

Author contributions: D.-C.T., T.G., Y.B., J.-D.F., S.D., H.F., M.J.B., L.L., and S.G. designed research; D.-C.T., J.L., T.G., Y.B., Q.D., V.V., F.T., M.L., U.V., J.-D.F., S.D., L.L., and S.G. performed research; D.-C.T., J.L., T.G., Y.B., M.L., P.G., J.-D.F., S.D., H.F., M.J.B., L.L., and S.G. analyzed data; and D.-C.T., T.G., Y.B., M.J.B., L.L., and S.G. wrote the paper.

The authors declare no conflict of interest.

This article is a PNAS Direct Submission.

Data deposition: PUCHI:GR expression data were deposited in the Gene Expression Omnibus (GEO) of the National Center for Biotechnology Information (NCBI) and are accessible through GEO accession no. GSE128721, https://www.ncbi.nlm.nih.gov/geo.

[1]To whom correspondence may be addressed. Email: laurent.laplaze@ird.fr or soazig.guyomarch@ird.fr.

This article contains supporting information online at www.pnas.org/lookup/suppl/doi:10.1073/pnas.1906300116/-/DCSupplemental.

Published online June 24, 2019.

encode two HACD enzymes (24), while the product of the *ENOYL CO-A REDUCTASE/ECERIFERUM 10* (*ECR/CER10*) gene has ECR activity (25). These enzymes are physically linked together by PASTICCINO 1 (PAS1; ref. 26). VLCFAs are components of various classes of membrane, storage, and extracellular lipids (26). VLCFA-containing sphingolipids and glycerolipids provide unique properties to membranes promoting interleaflet interactions and lipid rafts formation. As such, VLCFAs influence membrane dynamics during cell division (27, 28), the distribution of membrane proteins such as auxin transporters (29, 30), and are involved in noncell-autonomous processes of growth regulation (31–33). In addition, VLCFA-containing lipids, or their derivatives, are thought to act as second messengers in response to various stimuli (34, 35). Finally, VLCFAs are components of hydrophobic extracellular material such as skin barriers in mammals (36) or suberin and cuticular waxes in plants (26).

In this study, we identified genes acting downstream of PUCHI using a time course LR transcriptomic dataset (37) combined with a gene regulatory network (GRN) inference algorithm (17). We found PUCHI-dependent expression of genes involved in the biosynthesis of VLCFAs during LR development. Consistently, VLCFA mutants display defects in LR development similar to *puchi-1*. VLCFAs were previously described to regulate the competence of pericycle cells to generate calli on an auxin-rich callus-inducing medium (CIM) (33). We show that PUCHI is also expressed in CIM-treated roots and regulates the expression of genes involved in VLCFA biosynthesis during CIM-induced callus formation. Accordingly, CIM-treated roots of the *puchi-1* mutant show a reduced level of VLCFAs compared with wild type and exhibit comparable phenotype to VLCFA biosynthesis mutants. Our results indicate that PUCHI-regulated VLCFA biosynthesis is part of a pathway controlling cell proliferation during LR and callus formation.

Results

PUCHI Regulates VLCFA Biosynthesis Genes during Lateral Root Development. To gain insight into the function(s) of PUCHI during LR development, we took advantage of the time-course transcriptomic dataset profiling every stage of LRP organogenesis (37) to identify candidate genes whose expression is regulated by this transcription factor. We employed the TDCor algorithm (17) to search the LR dataset (38) for genes exhibiting an expression profile highly similar to that of *PUCHI* (Pearson's correlation coefficient > 0.80) when shifted back in time by 3 h. Our in silico analysis retrieved 217 potential target genes whose expression profiles are correlated with that of *PUCHI* (*SI Appendix*, Table S1). A Gene Ontology (GO) enrichment analysis using BiNGO (39) revealed that 71 GO biological processes were significantly overrepresented in this group of putative downstream genes (*SI Appendix*, Table S2). Among them, the "VLCFA biosynthesis" category stood out as one of the most strongly overrepresented biological processes ($P = 0.006$). In the LR dataset, *PUCHI* transcript abundance rapidly rises after LR induction and peaks at around 12 h after gravistimulation, which corresponds to the time when the first round of anticlinal cell division is observed (Fig. 1*A*, black line). *PUCHI* transcript levels then gradually decrease over time. Expression profiles of genes encoding key enzymes for each step of the VLCFA elongation cycle displayed comparable dynamics, albeit shifted in time. These included *KCS1*, *KCS2*, *KCS9*, *KCS17*, and *KCS20* genes, all encoding members of the KCS enzyme family catalyzing the first step of VLCFA elongation, as well as *KCR1*, *PAS2*, and *ECR/CER10*, which encode enzymes catalyzing the second, third, and fourth steps of VLCFA elongation, respectively, and *PAS1* (Fig. 1*A* and *SI Appendix*, Fig. S2).

We validated this inference approach with a classical transcriptomic analysis of the *puchi-1* mutant complemented with a dexamethasone (DEX) inducible PUCHI-GLUCOCORTICOID RECEPTOR (GR) protein fusion expressed under the control of

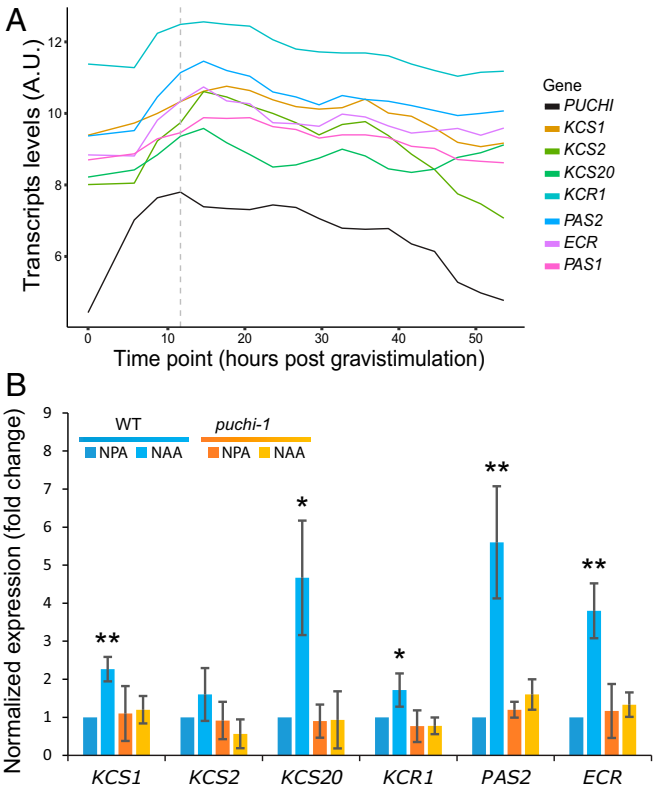

Fig. 1. VLCFA biosynthesis genes are induced during LRP development in a PUCHI-dependent manner. (*A*) Transcripts accumulation levels are expressed in arbitrary units (A.U.). The gray dotted line indicates the time point when *PUCHI* expression reaches a maximum after LR induction. (*B*) VLCFA biosynthetic gene expression by RT-qPCR in WT (blue) and *puchi-1* roots (orange). Lateral root formation is inhibited in control plants treated with NPA (darker shade), while on NAA (brighter shade) lateral root initiation is induced synchronously along the primary root in both WT and *puchi-1*. Roots were harvested after 24 h treatment on 5 μM NPA or 10 μM NAA. Normalization was achieved with the *CYCLIN-DEPENDENT KINASE A;1* (*CDKA;1*) gene. The calibrator cDNA is WT under NPA treatment. Data are represented as mean ± SEM of three biological replicates. Significance was determined by Student's *t* test (*$P < 0.05$, **$P < 0.01$).

the *PUCHI* promoter. Treatment of *pPUCHI::PUCHI:GR/puchi-1* seedlings with DEX targets the recombinant transcription factor to the nucleus to regulate gene expression (40, 41) and restore the WT LR phenotype (*SI Appendix*, Fig. S3). We used the auxin naphthaleneacetic acid (NAA) to induce LR formation and, therefore, increase the number of cells in which the PUCHI promoter is activated (42). Forty-six genes were significantly regulated (fold change >1.5 and $P < 0.05$) after 4 h NAA + DEX treatment compared with NAA alone. Only four of these genes were common with the genes recovered from our in silico analysis including one gene involved in VLCFA biosynthesis (*KCS8*), thus supporting activation of VLCFA biosynthesis genes downstream of PUCHI. However, this activation was lost when cycloheximide was added (*SI Appendix*, Table S3). Hence, while expression of a set of genes encoding for the entire VLCFA elongation pathway was stimulated in a PUCHI-dependent manner during LR formation, these genes were not primary targets of PUCHI.

To confirm the PUCHI-dependent activation of the VLCFA biosynthesis pathway during LR development, we compared expression levels of VLCFA biosynthesis genes in WT and *puchi-1* roots during LR formation by RT-qPCR. An auxin-dependent LR induction system (LRIS, modified from ref. 43; *SI Appendix*, Fig. S4) was used to synchronously induce lateral root formation along the whole primary root. Transcript levels of *KCS1*, *KCS2*,

KCS20, *KCR1*, *PAS2*, and *ECR*/*CER10* were elevated after LR induction by NAA treatment in WT, but this response was disrupted in the *puchi-1* loss-of-function mutant background (Fig. 1*B*). Hence, genes encoding key components of the fatty acid elongase complex responsible for VLCFA biosynthesis are induced during LRP development, and this is dependent on the PUCHI transcription factor.

PUCHI Controls the Spatial Expression of VLCFA Biosynthesis Genes during LR Development. We next analyzed the spatial expression pattern of VLCFA biosynthesis genes during LR development using promoter-reporter gene fusions in WT and *puchi-1* backgrounds. A functional *pPUCHI::GFP:PUCHI* reporter is expressed throughout LRP during early stages of development, then the expression is excluded from the tip and limited to the flanks (Fig. 2*A*; ref. 18). The functional *pKCS1::KCS1:GFP* reporter was expressed in the outermost layer of cells in LRP (Fig. 2*B*). *KCS6*, *KCR1*, *PAS2*, and *PAS1* GUS reporter transgenes were strongly expressed in developing and emerging LRP (Fig. 2 *C* and *E*–*G*), whereas *pKCS20::GUS* was expressed in a few cells of LRP (Fig. 2*D*). Interestingly, these transgenes displayed distinct expression patterns in emerging LRP, with *pKCS6::GFP:GUS*, *pKCS20::GUS*, and *pPAS1::GUS* showing stronger activity at the base of emerging LRs (Fig. 2 *C*, *D*, and *G*), whereas expression of *pKCS1::KCS1:GFP*, *pKCR1::GFP:GUS*, and *pPAS2::GUS* was stronger at their tips (Fig. 2 *B*, *E*, and *F*).

When introgressed into the *puchi-1* background, we observed a clear reduction in *pKCS1::KCS1:GFP* and *pKCS6::GFP:GUS* expression in developing LRP (Fig. 2 *H* and *I*). In contrast, *pKCS6::GFP:GUS* and *pKCS20::GUS* expression was clearly enhanced in *puchi-1* emerging LRs, especially at their tips (Fig. 2*J*). Loss of function of PUCHI also caused a clear and consistent decrease in expression of *pKCR1::GFP:GUS*, *pPAS2::GUS*, and *pPAS1::GUS* in developing LRP and emerging LRs (Fig. 2 *K*–*M*). Interestingly, expression of these reporters became confined to several basal and flank cells in a majority of emerging LRs. These contrasted changes in reporter genes expression might not completely reflect the endogenous expression of the corresponding genes and suggest that feedbacks might occur. Nevertheless, our analyses confirmed that key VLCFA biosynthesis genes are expressed during LRP development and that their expression patterns in LRP are dependent on PUCHI.

PUCHI Inhibits LR Initiation but Is Necessary for Later Organ Development. To better understand the role of PUCHI during LRP development, we carefully characterized the impact of the *puchi-1* mutation on LR formation. Emerged LR and nonemerged LRP were counted along the primary root of 9-d-old seedlings (Fig. 3*A*). LRP located in the LR formation zone, i.e., rootwards of the most recently emerged LR, were scored as "developing LRP" (Fig. 3*A*, ref. 44). Although the density of emerged LR was not significantly different between *puchi-1* and WT, the density of developing LRP in the LR formation zone was almost three times higher in the mutant compared with WT (Fig. 3*B*). Consistent with this observation, the distances between two consecutive LRP were much shorter intervals in *puchi-1* than in WT with clusters of developing LRP either along a longitudinal (i.e., along a protoxylem pole) or radial (i.e., along opposite protoxylem poles) axis (Fig. 3 *C* and *D*, ref. 45). Thus, our data reveals that PUCHI represses LRP initiation in the pericycle and controls the spacing between LRP. This is consistent with recent results linking PUCHI to lateral inhibition of LR development by a peptide hormone-receptor signaling pathway (46).

In the root branching zone, i.e., shootward of the most recently emerged LRs (Fig. 3*A*, ref. 44), a strikingly high number of nonemerged LRP were present in the mutant, consistent with the observation of higher LRP initiation rate in the LRP formation zone (Fig. 3*B*). To test if they correspond to arrested or

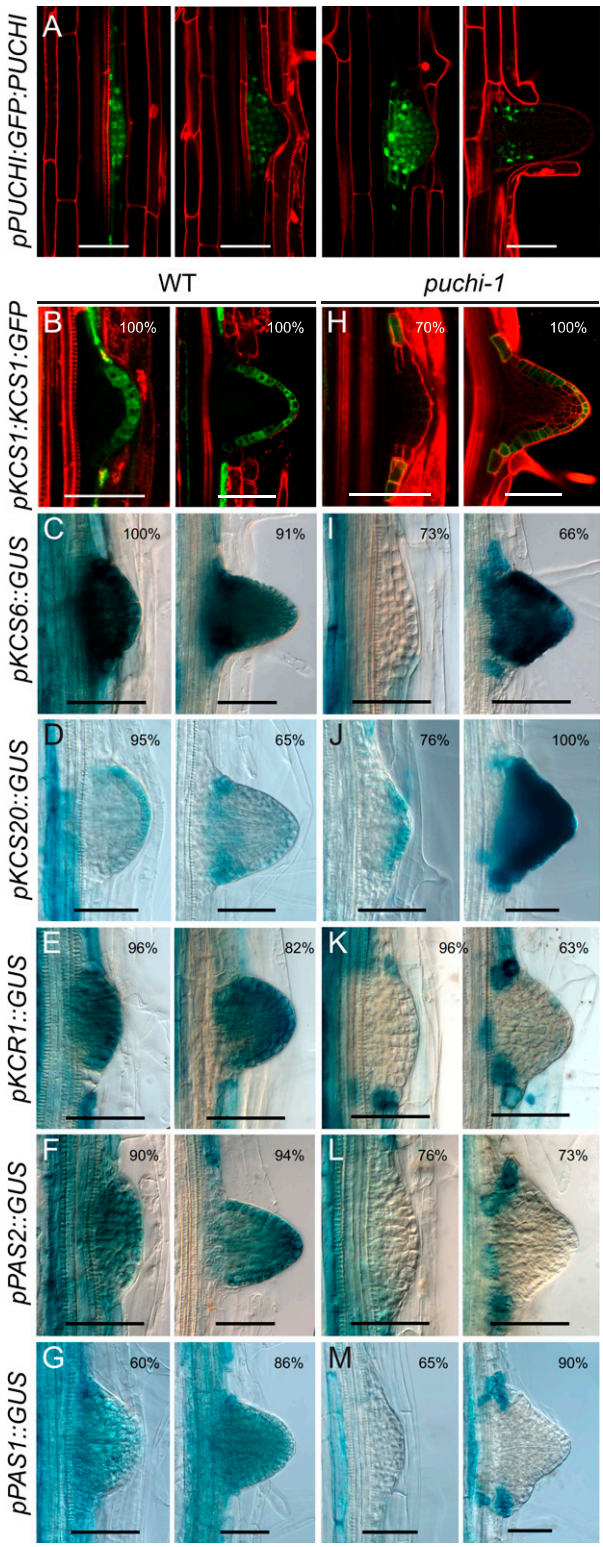

Fig. 2. VLCFA genes are expressed in developing LRP, and their expression patterns are dependent on PUCHI. (*A*) Expression of *pPUCHI::GFP:PUCHI* in *puchi-1* background is observed in developing LRP and is gradually confined to their base and flanks. (*B*–*M*) Expression patterns of various translational and transcriptional reporter constructs of VLCFA biosynthesis genes in typical WT (*B*–*G*) and *puchi-1* (*H*–*M*) LRP and newly emerged LR. (Scale bars: 50 μm.) Numbers indicate the percentage of LRP or LR displaying the corresponding expression pattern. n = 30–40 seedlings for each GUS assay.

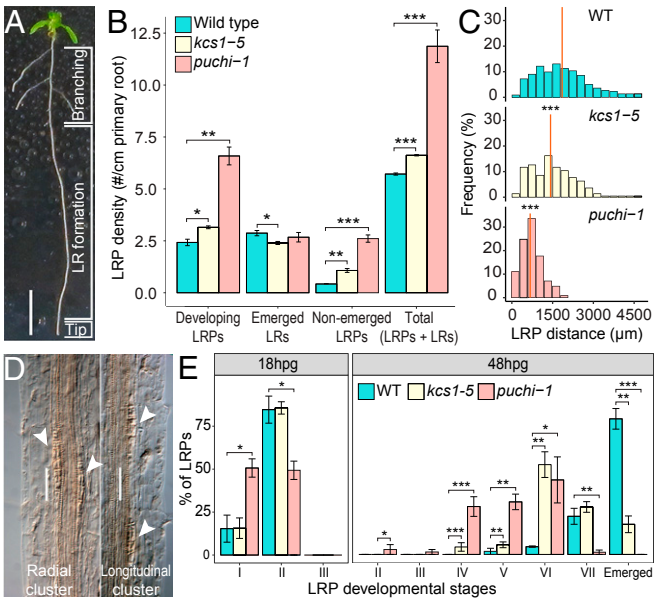

Fig. 3. LR initiation is enhanced but LRP development is delayed in *puchi-1* mutant. (*A*) Root branching events were scored in three distinct developmental zones of *Arabidopsis* primary root regarding lateral root formation as suggested in ref. 44. (*B*) Density of developing LRP, emerged LR, delayed LRP, and total LR initiations (LRP + LR) in 9-d-old WT, *puchi-1*, and *kcs1-5* seedlings. Developing LRP are LRP scored in the LR formation zone. Delayed LRP are defined as those located in the branching zone of the primary root but have not crossed the epidermis. Data are represented as mean ± SEM of three biological replicates; number of seedlings ≥20 in each repeat. Significance was determined by Student's *t* test. (*C*) Frequency distribution of distances between two consecutive LRP in WT, *kcs1-5*, and *puchi-1* roots. Each bin of the histogram represents a range of 300 μm. Number of LRP = 222, 208, and 228 for WT, *kcs1-5*, and *puchi-1*, respectively. The orange bar in each histogram indicates the mean LRP distance in each genotype. The asterisks in the histograms for *kcs1-5* and *puchi-1* indicate the significant difference between these mean distances compared with that of WT. (*D*) Examples of longitudinal and radial clusters of LRP in *puchi-1* roots. Arrowheads indicate LRP. (Scale bars: 50 μm.) (*E*) Distribution of developmental stages as described by Malamy and Benfey (5) achieved by gravistimulation-induced LRP formation in WT, *kcs1-5*, and *puchi-1* roots at 18 and 48 h after the gravistimulation. Data are represented as mean ± SEM of three biological replicates, with number of seedlings ≥20 in each repeat. For all occasions, $*P < 0.05$, $**P < 0.01$, $***P < 0.001$.

delayed LRP, we marked and counted the number of emerged LRP in the root branching zone first 9 d after germination and then again after four extra days of growth. In both WT and *puchi-1*, we observed that none or very few new LRs had emerged during these additional days, consistent with the hypothesis that these nonemerged LRP have stopped developing (*SI Appendix*, Table S4). Thus, our data suggest that in addition to LRP initiation density, loss of *PUCHI* function also impacts LRP development. To confirm this, we used a gravistimulation-based LR induction system (47, 48) to analyze the kinetics of LRP development in *puchi-1* compared with WT and scored the developmental stages reached by LRP (5) 18 and 48 h after induction (Fig. 3*E*). Gravistimulation induced the initiation of LRP development in almost 100% of the *puchi-1* and WT seedlings. However, a delay in *puchi-1* LRP development was already observed 18 h after gravistimulation compared with WT. At 48 h, a majority of WT LRP had emerged while most *puchi-1* LRP only reached developmental stages IV, V, or VI (Fig. 3*E*). Six days after gravistimulation, 100% (53/53) of induced LRP had emerged in the WT background, whereas only 70% (35/50) did so in the *puchi-1* background. Hence, PUCHI is required for normal developmental progression of LRP and LR emergence.

VLCFA Mutants Display Similar Defects in Lateral Root Development as *Puchi-1*. We performed the same lateral root phenotyping assay for VLCFA mutants. We focused on mutants in *KCS* genes expressed downstream of PUCHI during lateral root development (*kcs1-5*, *kcs9*, *kcs2 kcs20*), and *ECR*/*CER10* genes because (*i*) mutants in *KCR1*, *PAS1*, and *PAS2* display severe and pleiotropic developmental phenotypes (22, 23), (*ii*) loss-of-function phenotype for those *KCS* and *ECR* genes have been described (21, 25, 29, 33, 49), and (*iii*) functional redundancy and substrate specificity of KCS enzymes have been studied (21, 50). We did not observe any significant differences in LRP formation and development between *kcs9* single mutants nor *kcs2 kcs20* double mutant and WT seedlings. However, *kcs1-5* mutant, a null allele for the *KCS1* gene (33), displayed a root branching phenotype similar to *puchi-1*, albeit milder (Fig. 3 *B*–*E*). An *ECR* mutant (*cer10-2*) produced similar but weaker phenotype (*SI Appendix*, Fig. S5). Moreover, double *kcs1-5 kcs20* and *kcs1-5 cer10-2* mutants resulted in more pronounced LRP development defects compared with the corresponding single mutants (*SI Appendix*, Fig. S6). Hence, VLCFA biosynthesis loss-of-function mutants exhibited similar defects in LRP development as *puchi-1*. These defects were weaker than those observed in *puchi-1*, possibly due to the fact that PUCHI may simultaneously regulate multiple VLCFA genes and possibly other pathways, and that VLCFA enzymes may act redundantly as indicated by our double mutant analysis.

PUCHI and VLCFAs Control Pericycle Cell Proliferation on Callus Inducing Medium. VLCFAs were recently shown to control the ability of pericycle cells to form calli in *Arabidopsis* roots (33). This prompted us to investigate the role of PUCHI during callus formation. When 7-d-old *pPUCHI::GFP:PUCHI* seedlings were incubated on CIM, reporter gene expression was observed in developing calli (Fig. 4*A*). Before being transferred to CIM, WT and *puchi-1* roots displayed comparable anatomy (Fig. 4 *B*, *Upper*). After 4 d on CIM, both WT and *puchi-1* roots responded to the hormonal treatment with pericycle cell proliferation (Fig. 4 *B*, *Lower*). However, whereas WT roots produced dome-shaped calli, the *puchi-1* mutant generated a continuous layer of dividing cells along its entire primary root. This phenotype was similar and stronger than the fused-calli phenotype displayed by the VLCFA biosynthesis-deficient mutant *kcs1-5* (Fig. 4*B* and *SI Appendix*, Fig. S7; ref. 33). DEX treatment restored a WT callus formation phenotype in *pPUCHI::PUCHI:GR*/*puchi-1* plants on CIM medium (Fig. 4*C*), thus confirming that the callus formation phenotype of *puchi-1* roots on CIM is caused by loss of function of *PUCHI*. We next analyzed if PUCHI is required for the expression of VLCFA genes in the context of CIM-induced callus formation. *pKCS1::KCS1:GFP*, *pKCS6::GFP:GUS*, and *pKCR1::GFP:GUS* expression were studied after CIM treatment in WT and *puchi-1* backgrounds. All three reporter genes were expressed in calli in WT plants, and this expression was lost in *puchi-1* (*SI Appendix*, Fig. S8). Hence, PUCHI and VLCFAs restrict pericycle cell proliferation during callus formation and PUCHI is necessary for expression of VLCFA biosynthesis genes in response to CIM treatment.

***Puchi-1* Displays Altered VLCFA Content.** To further demonstrate that the *puchi-1* phenotypes were linked to changes in VLCFA content, we analyzed the fatty acid composition in WT, *kcs1-5*, and *puchi-1* CIM-treated roots. CIM treatment was chosen because of the strong associated phenotypes and as it generated a large amount of material for lipidomics. The total amount of fatty acids was similar in all three lines, but the amount and proportion of VLCFAs were significantly lower in *kcs1-5* and *puchi-1* compared with WT (Fig. 4*D* and *SI Appendix*, Fig. S9).

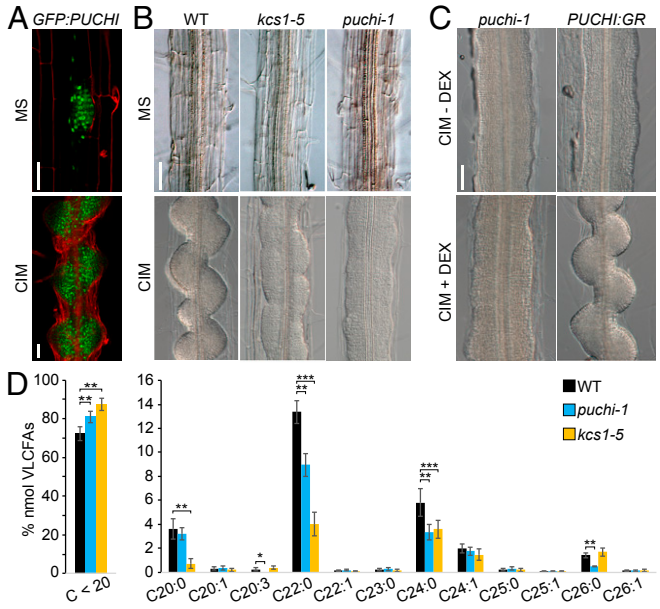

Fig. 4. Callus formation is enhanced in *puchi-1* roots. (*A*) *pPUCHI::GFP:PUCHI* expression in calli induced by CIM. (*B*) Seven-day-old *puchi-1, kcs1-5,* and WT seedlings grown on 1/2 MS medium (*Upper*), and after four more days of growth on CIM (*Lower*). (*C*) *pPUCHI::PUCHI:GR/puchi-1* plus DEX restores callus formation in *puchi-1* roots on CIM. $n = 40$ for WT, *kcs1-5*, and *puchi-1*. $n = 20$ for *pPUCHI::PUCHI:GR/puchi-1*. (*D*) Global fatty acids of WT, *puchi-1*, and *kcs1-5* roots after 4 d on CIM. The results are the sum of carboxylic acids, α,ω-dicarboxylic acids, ω-hydroxy acids, fatty alcohols, and two-hydroxy fatty acids. Data are represented as mean ± SEM of six, six, and five biological replicates for WT, *puchi-1*, and *kcs1-5*, respectively. $*P < 0.05$, $**P < 0.01$, $***P < 0.001$. (Scale bars: *A*, 50 μm; *B* and *C*, 0.1 mm.)

Interestingly, a detailed analysis showed that C22 fatty alcohols (22:0-OH) and C24 sphingolipids (h24:0) were significantly reduced in *puchi-1* while precursors (C16, C18) were more abundant (*SI Appendix*, Fig. S10). VLCFAs are precursors of suberin and cutin biosynthesis. A suberin and cutin-like layer was recently described overlying developing LRP (51, 52). Suberin and root cutin are composed from dicarboxylic acid (DCA), ω-hydroxy acids (ωOH), and fatty alcohols (OH) (52, 53). The level of all C18-containing fatty acids typical of suberin/cutin (ωOH-18, 18-DCA, and 18-OH) was similar between *puchi* and WT (*SI Appendix*, Fig. S10). However, we cannot exclude qualitative changes in composition of the suberin/cutin layer in front of LRP that would be regulated by PUCHI.

Discussion

We report that spatiotemporal expression of genes encoding VLCFA biosynthetic enzymes is coordinately regulated by PUCHI during LR formation. Interestingly, while expression of nonredundant *KCR1*, *PAS2*, and *PAS1* genes (54, 55) is induced by PUCHI throughout developing LRP in a similar manner, partially redundant *KCS* genes involved in the biosynthesis of VLCFAs of various chain lengths (21, 50, 55) displayed more diverse expression patterns and regulation. Our data suggest that VLCFAs of specific chain lengths may be synthesized and required in different cell types and/or at different stages of LRP development where they might contribute to LRP patterning.

The *puchi-1* loss-of-function mutant has been reported to exhibit LRP with abnormal cell division patterns and with higher cell proliferation rates compared with WT at the organ flanks (18). We report a delay in LRP development and emergence, as well as higher initiation density along the primary root, with frequent clustering of primordia under both normal and tissue culture (CIM) conditions. This is consistent with previous studies indicating that VLCFAs are important to restrict cell proliferation (31). It was recently shown that VLCFA biosynthesis was also necessary to organize cell proliferation into distinct calli in *Arabidopsis* roots grown on CIM (33). Importantly, callus formation shares common steps with the LRP formation pathway (12–14). We showed here that the *puchi-1* mutation causes roots to form a fused and continuous calli when treated with CIM, a phenotype reminiscent and even stronger than the one reported for *kcs1-5* and other mutants (33). Interestingly, roots of *puchi-1* and VLCFA mutants produced more LRP than WT roots, and these LRP exhibit ectopic cell divisions, suggesting that PUCHI regulates a pathway restricting pericycle cell proliferation that is conserved between LR development and in vitro callus formation. Given that defects in VLCFA biosynthesis lead to cell overproliferation in different contexts such as shoot vasculature (31, 56), CIM-induced calli (ref. 33; this study), and in LRP (29), the regulation of VLCFA biosynthesis genes by PUCHI may explain part of the *puchi-1* LRP and CIM phenotype. PUCHI-regulated VLCFA biosynthesis might also be critical for cell patterning in lateral root primordia as evidenced by *puchi-1* phenotype and specific expression profiles of individual VLCFA biosynthesis genes. Further experiments will be needed to test this interesting hypothesis.

VLCFAs could regulate cell proliferation in several ways. VLCFAs can be incorporated into cell membranes and influence their structural and functional dynamics, especially endocytosis, vesicular trafficking, and exocytosis, impacting cell cytokinesis or the targeting to the membrane of important factors, such as auxin transporters (27, 29, 30). More generally, VLCFA content and composition may modulate hormonal signaling dynamics, especially cytokinins and auxins (31, 57). Last, VLCFA distribution could impact the mechanical properties of the tissues by modifying cell wall composition in the endodermis (22) or tissues that overlay LRP (51).

In conclusion, using a systems biology approach we found that the expression of multiple important enzymes catalyzing each of the four steps of the VLCFA elongation cycle are up-regulated during LRP development, and this is dependent on the AP2/EREPB transcription factor PUCHI. In addition, the *puchi-1* loss-of-function mutant shares similar LRP and callus phenotypes with mutants impaired in VLCFA biosynthesis. Hence, during root branching and root-derived callus formation, the PUCHI transcription factor stimulates the expression of key VLCFA biosynthesis genes to regulate cell proliferation, organogenesis, and organ spacing.

Materials and Methods

Plant materials, transgenic plant generation, plant growth conditions, and methods for root phenotyping, microscopy and cytological analyses, transcriptome and gene expression level analyses, callus formation assay, and lipidomics profiling by gas chromatography-mass spectrometry (GC-MS) are described in *SI Appendix, SI Materials and Methods*. Primers used are listed in *SI Appendix*, Table S5. PUCHI-GR expression data were deposited in the Gene Expression Omnibus of the National Center for Biotechnology Information under accession no. GSE128721.

ACKNOWLEDGMENTS. We thank Dr. M. Devic and Dr. T. Roscoe (CNRS) for helpful discussions and critical reading of the manuscript. This work was supported by the Institute of Research for Development, the University of Montpellier, the University of Science and Technology of Hanoi and the French Embassy in Hanoi (Ph.D. grant to D.-C.T.), the ENS Paris (PhD grant to J.L.) and the French National Research Agency (ANR) through NewRoot project Grant ANR-17-CE13-0004-01 (to M.L., L.L. and S.G.). U.V., and M.J.B. acknowledge the support of the Biological and Biotechnology Science Research Council (BBSRC) and Engineering and Physical Sciences Research Council funding to the Centre for Plant Integrative Biology from Grant BB/D019613/1 and BBSRC Grant BB/H020314/1. The Institut Jean-Pierre Bourgin benefits from support from the LabEx Saclay Plant Sciences-SPS Grant

ANR-10-LABX-0040-SPS. Lipidomic analyses were performed on the Bordeaux Metabolome Facility-MetaboHUB via Grant ANR-11-INBS-0010. H.F. was supported by Grant-in-Aid 19060006 for Scientific Research on Priority Areas and Grant-in-Aid 25110330 for Scientific Research on Innovative Areas.

1. E. C. Morris *et al*., Shaping 3D root system architecture. *Curr. Biol.* **27**, R919–R930 (2017).
2. S. Smith, I. De Smet, Root system architecture: Insights from arabidopsis and cereal crops. *Philos. Trans. R. Soc. Lond. B Biol. Sci.* **367**, 1441–1452 (2012).
3. A. Zhan, H. Schneider, J. P. Lynch, Reduced lateral root branching density improves drought tolerance in maize. *Plant Physiol.* **168**, 1603–1615 (2015).
4. B. K. Möller, W. Xuan, T. Beeckman, Dynamic control of lateral root positioning. *Curr. Opin. Plant Biol.* **35**, 1–7 (2017).
5. J. E. Malamy, P. N. Benfey, Organization and cell differentiation in lateral roots of Arabidopsis thaliana. *Development* **124**, 33–44 (1997).
6. M. Lucas *et al*., Lateral root morphogenesis is dependent on the mechanical properties of the overlaying tissues. *Proc. Natl. Acad. Sci. U.S.A.* **110**, 5229–5234 (2013).
7. D. von Wangenheim *et al*., Rules and self-organizing properties of post-embryonic plant organ cell division patterns. *Curr. Biol.* **26**, 439–449 (2016).
8. T. Goh *et al*., Quiescent center initiation in the Arabidopsis lateral root primordia is dependent on the SCARECROW transcription factor. *Development* **143**, 3363–3371 (2016).
9. D. Stoeckle, M. Thellmann, J. E. Vermeer, Breakout-lateral root emergence in Arabidopsis thaliana. *Curr. Opin. Plant Biol.* **41**, 67–72 (2018).
10. J. Lavenus, M. Lucas, L. Laplaze, S. Guyomarc'h, The dicot root as a model system for studying organogenesis. *Methods Mol. Biol.* **959**, 45–67 (2013).
11. J. Perianez-Rodriguez, C. Manzano, M. A. Moreno-Risueno, Post-embryonic organogenesis and plant regeneration from tissues: Two sides of the same coin? *Front. Plant Sci.* **5**, 219 (2014).
12. M. Fan, C. Xu, K. Xu, Y. Hu, LATERAL ORGAN BOUNDARIES DOMAIN transcription factors direct callus formation in Arabidopsis regeneration. *Cell Res.* **22**, 1169–1180 (2012).
13. K. Sugimoto, Y. Jiao, E. M. Meyerowitz, Arabidopsis regeneration from multiple tissues occurs via a root development pathway. *Dev. Cell* **18**, 463–471 (2010).
14. R. Atta *et al*., Pluripotency of Arabidopsis xylem pericycle underlies shoot regeneration from root and hypocotyl explants grown in vitro. *Plant J.* **57**, 626–644 (2009).
15. C. D. Trinh, L. Laplaze, S. Guyomarc'h, "Lateral Root Formation: Building a Meristem de novo" in *Annual Plant Reviews*, J. A. Roberts Ed. (John Wiley & Sons, 2018), pp. 1–44.
16. Y. Du, B. Scheres, Lateral root formation and the multiple roles of auxin. *J. Exp. Bot.* **69**, 155–167 (2018).
17. J. Lavenus *et al*., Inference of the Arabidopsis lateral root gene regulatory network suggests a bifurcation mechanism that defines primordia flanking and central zones. *Plant Cell* **27**, 1368–1388 (2015).
18. A. Hirota, T. Kato, H. Fukaki, M. Aida, M. Tasaka, The auxin-regulated AP2/EREBP gene PUCHI is required for morphogenesis in the early lateral root primordium of Arabidopsis. *Plant Cell* **19**, 2156–2168 (2007).
19. J. Joubès *et al*., The VLCFA elongase gene family in Arabidopsis thaliana: Phylogenetic analysis, 3D modelling and expression profiling. *Plant Mol. Biol.* **67**, 547–566 (2008).
20. A. A. Millar, L. Kunst, Very-long-chain fatty acid biosynthesis is controlled through the expression and specificity of the condensing enzyme. *Plant J.* **12**, 121–131 (1997).
21. J. Kim *et al*., Arabidopsis 3-ketoacyl-coenzyme a synthase9 is involved in the synthesis of tetracosanoic acids as precursors of cuticular waxes, suberins, sphingolipids, and phospholipids. *Plant Physiol.* **162**, 567–580 (2013).
22. F. Beaudoin *et al*., Functional characterization of the Arabidopsis beta-ketoacyl-coenzyme A reductase candidates of the fatty acid elongase. *Plant Physiol.* **150**, 1174–1191 (2009).
23. L. Bach *et al*., The very-long-chain hydroxy fatty acyl-CoA dehydratase PASTICCINO2 is essential and limiting for plant development. *Proc. Natl. Acad. Sci. U.S.A.* **105**, 14727–14731 (2008).
24. C. Morineau *et al*., Dual fatty acid elongase complex interactions in arabidopsis. *PLoS One* **11**, e0160631 (2016).
25. H. Zheng, O. Rowland, L. Kunst, Disruptions of the Arabidopsis Enoyl-CoA reductase gene reveal an essential role for very-long-chain fatty acid synthesis in cell expansion during plant morphogenesis. *Plant Cell* **17**, 1467–1481 (2005).
26. Y. Li-Beisson *et al*., Acyl-lipid metabolism. *Arabidopsis Book* **11**, e0161 (2013).
27. L. Bach *et al*., Very-long-chain fatty acids are required for cell plate formation during cytokinesis in Arabidopsis thaliana. *J. Cell Sci.* **124**, 3223–3234 (2011).
28. D. Molino *et al*., Inhibition of very long acyl chain sphingolipid synthesis modifies membrane dynamics during plant cytokinesis. *Biochim. Biophys. Acta* **1841**, 1422–1430 (2014).
29. F. Roudier *et al*., Very-long-chain fatty acids are involved in polar auxin transport and developmental patterning in Arabidopsis. *Plant Cell* **22**, 364–375 (2010).
30. V. Wattelet-Boyer *et al*., Enrichment of hydroxylated C24- and C26-acyl-chain sphingolipids mediates PIN2 apical sorting at trans-Golgi network subdomains. *Nat. Commun.* **7**, 12788 (2016).
31. T. Nobusawa *et al*., Synthesis of very-long-chain fatty acids in the epidermis controls plant organ growth by restricting cell proliferation. *PLoS Biol.* **11**, e1001531 (2013).
32. T. Yamauchi *et al*., Ethylene biosynthesis is promoted by very-long-chain fatty acids during lysigenous aerenchyma formation in rice roots. *Plant Physiol.* **169**, 180–193 (2015).
33. B. Shang *et al*., Very-long-chain fatty acids restrict regeneration capacity by confining pericycle competence for callus formation in *Arabidopsis*. *Proc. Natl. Acad. Sci. U.S.A.* **113**, 5101–5106 (2016).
34. A. Poulos, Very long chain fatty acids in higher animals–A review. *Lipids* **30**, 1–14 (1995).
35. A. De Bigault Du Granrut, J.-L. Cacas, How very-long-chain fatty acids could signal stressful conditions in plants? *Front. Plant Sci.* **7**, 1490 (2016).
36. A. Kihara, Very long-chain fatty acids: Elongation, physiology and related disorders. *J. Biochem.* **152**, 387–395 (2012).
37. U. Voß *et al*., The circadian clock rephases during lateral root organ initiation in Arabidopsis thaliana. *Nat. Commun.* **6**, 7641 (2015).
38. U. Voß *et al*., Data from "CPIB Lateral Root timecourse." ArrayExpress. https://www.ebi.ac.uk/arrayexpress/experiments/E-MTAB-2565. Deposited 1 February 2015.
39. S. Maere, K. Heymans, M. Kuiper, BiNGO: A Cytoscape plugin to assess overrepresentation of gene ontology categories in biological networks. *Bioinformatics* **21**, 3448–3449 (2005).
40. M. Schena, A. M. Lloyd, R. W. Davis, A steroid-inducible gene expression system for plant cells. *Proc. Natl. Acad. Sci. U.S.A.* **88**, 10421–10425 (1991).
41. T. Aoyama, N. H. Chua, A glucocorticoid-mediated transcriptional induction system in transgenic plants. *Plant J.* **11**, 605–612 (1997).
42. T. Goh, H. Fukaki. Data from "Profiling downstream targets of PUCHI in roots of Arabidopsis thaliana." Gene Expression Omnibus. https://www.ncbi.nlm.nih.gov/geo/query/acc.cgi?acc=GSE128721. Deposited 22 March 2019.
43. K. Himanen *et al*., Transcript profiling of early lateral root initiation. *Proc. Natl. Acad. Sci. U.S.A.* **101**, 5146–5151 (2004).
44. J. G. Dubrovsky, B. G. Forde, Quantitative analysis of lateral root development: Pitfalls and how to avoid them. *Plant Cell* **24**, 4–14 (2012).
45. H. Hofhuis *et al*., Phyllotaxis and rhizotaxis in Arabidopsis are modified by three PLETHORA transcription factors. *Curr. Biol.* **23**, 956–962 (2013).
46. K. Toyokura *et al*., Lateral inhibition by a peptide hormone-receptor cascade during arabidopsis lateral root founder cell formation. *Dev. Cell* **48**, 64–75.e5 (2018).
47. M. Lucas, C. Godin, C. Jay-Allemand, L. Laplaze, Auxin fluxes in the root apex co-regulate gravitropism and lateral root initiation. *J. Exp. Bot.* **59**, 55–66 (2008).
48. B. Péret *et al*., Auxin regulates aquaporin function to facilitate lateral root emergence. *Nat. Cell Biol.* **14**, 991–998 (2012).
49. S. B. Lee *et al*., Two Arabidopsis 3-ketoacyl CoA synthase genes, KCS20 and KCS2/DAISY, are functionally redundant in cuticular wax and root suberin biosynthesis, but differentially controlled by osmotic stress. *Plant J.* **60**, 462–475 (2009).
50. D. K. Kosma *et al*., AtMYB41 activates ectopic suberin synthesis and assembly in multiple plant species and cell types. *Plant J.* **80**, 216–229 (2014).
51. B. Li *et al*., Role of LOTR1 in nutrient transport through organization of spatial distribution of root endodermal barriers. *Curr. Biol.* **27**, 758–765 (2017).
52. A. Berhin *et al*., The root cap cuticle: A cell wall structure for seedling establishment and lateral root formation. *Cell* **176**, 1367–1378.e8 (2019).
53. C. Delude *et al*., Primary fatty alcohols are major components of suberized root tissues of arabidopsis in the form of alkyl hydroxycinnamates. *Plant Physiol.* **171**, 1934–1950 (2016).
54. L. Bach, J. D. Faure, Role of very-long-chain fatty acids in plant development, when chain length does matter. *C. R. Biol.* **333**, 361–370 (2010).
55. T. M. Haslam, L. Kunst, Extending the story of very-long-chain fatty acid elongation. *Plant Sci.* **210**, 93–107 (2013).
56. Y. Bellec *et al*., Pasticcino2 is a protein tyrosine phosphatase-like involved in cell proliferation and differentiation in Arabidopsis. *Plant J.* **32**, 713–722 (2002).
57. Y. Harrar, Y. Bellec, C. Bellini, J. D. Faure, Hormonal control of cell proliferation requires PASTICCINO genes. *Plant Physiol.* **132**, 1217–1227 (2003).